4ICEGE Thessaloniki-GREECE 2007

4th International Conference on
Earthquake Geotechnical Engineering
June 25-28, 2007
Paper No. 1173

# CHARACTERISTIC BEHAVIOR OF LIQUEFIABLE GROUNDS WITH LOW PERMEABILITY SUBLAYERS

**Mahmood SEID-KARBASI [1] and Peter M. BYRNE[2]**

## ABSTRACT

Prediction of liquefaction induced displacements and ground failure remains a great challenge in earthquake geotechnical engineering. Our insights into the problem have improved during the past decades based on data from past earthquakes, experimental laboratory studies, physical model tests and numerical analyses. However, the basis of our predictions is flawed as the majority of studies to date have been conducted with the assumption of undrained condition during earthquakes with no accounting for flow conditions. From these studies it is found that strengths based on undrained conditions are very much higher than residual strengths back calculated from field data.

Observations from past earthquakes and recent studies including physical model tests and numerical analyses have shown that flow conditions arising from the presence of low permeability sub-layers, have a very significant impact on liquefiable grounds deformations.

In this paper, a coupled stress-flow dynamic analysis procedure using an elastic-plastic constitutive model has been employed to explore the effects of a low permeability sub-layer on characteristic behavior of liquefiable deposits. It is shown that the barrier layer impedes the flow of water during and after earthquake shaking causing an expansion in the upper parts beneath the barrier while contraction occurs in the lower parts of the liquefiable layer, resulting in void redistribution. This behavior is largely controlled by flow boundary conditions and is independent of soil layer thickness. The expansion of the soil skeleton accounts for the low residual strengths observed from field case histories.

*Keywords:* liquefaction, flow slides, residual strength, void redistribution, silt barrier, UBCSAND

## INTRODUCTION

Earthquakes have caused severe damage to civil engineering structures, particularly where soil liquefaction was involved. Liquefaction can occur in granular soils whose pore spaces are filled with water, and involves generation of high pore water pressures and large reductions in soil shear stiffness and strength that can lead to very large shear deformations and failures.

Experience from past earthquakes indicates that liquefaction induced lateral spreads and flow slides have taken place in earth structures and foundations and also in coastal and river areas in many regions of the world including Alaska, 1964, Niigata, 1964 and Turkey, 1999. Movements may exceed several meters even in gentle slopes of less than a few percent (e.g. Hamada, 1992). Submarine slides have been seismically triggered in many regions as reported by Scott and Zukerman (1972) and Hamada (1992). More interestingly, flow slides have occurred not only during, but also

[1] Geotechnical Engineer, Golder Associates Ltd. Burnaby, BC, Canada,
Email: Mahmood_SeidKarbasi@golder.com.
[2] Professor emeritus, Civil Engineering Dept., University of British Columbia, BC. Canada,
Email: pmb@civil.ubc.ca.

after earthquake shaking. These large movements are mainly driven by gravity, although initially triggered to liquefy by seismic stresses.

Two key factors controlling the response of a liquefiable layer to an earthquake are:

- Mechanical conditions
- Flow conditions

Mechanical conditions i.e. soil density, stiffness and strength, static stress state, and earthquake characteristics (amplitude, duration, etc.) are mostly responsible for generation of excess pore pressure during cyclic loading. Flow conditions i.e. drainage path, soil permeability and its variation (permeability contrast) within the soil deposit control excess pore pressure redistribution during and after the earthquake. Sharp et al. (2003) and Seid-Karbasi & Byrne (2006a) using centrifuge model tests and numerical method respectively, demonstrated that liquefiable soil deposits with lower permeability suffer greater deformations in an earthquake. Seid-Karbasi & Byrne (2006a) also showed that pore water migration is responsible for liquefaction onset commonly observed first at shallower depths of uniform soil layers in past earthquakes and physical model tests.

The majority of the previous liquefaction studies are based on the assumption that no flow occurs during or after earthquake loading and were centered on mechanical conditions. However, this condition may not represent the real situation, because during and after shaking, water migrates from zones with higher excess pore pressure towards zones with lower excess pressure. Recent studies including field investigation (e.g. Kokusho & Kojima, 2002), physical model testing (e.g. Elgamal et al., 1986; Kukosho, 1999; Kokusho, 2003 and Kulasingam et al., 2004), and numerical analysis (e.g. Yang & Elgamal, 2002; Seid-Karbasi & Byrne, 2004a and Seid-Karbasi, 2007) showed that low permeability sub-layers are the cause of flow failures when relative densities exceed about 25%. The presence of such layers impedes the upward flow of water resulting in a very loose zone at the base of layers which leads to significant strength loss and post-shaking failure. This mechanism called “void redistribution” leads to a contracting zone in the lower parts of a sand layer while the upper parts are expanding. This expansion of the soil skeleton accounts for the low residual strengths observed from field case histories. The strength loss due to expansion can lead to failures even in very gentle slopes.

This paper presents the results of a study on the effects of thickness of liquefiable layer on this mechanism. The study is based on a coupled stress-flow dynamic analysis procedure and employing an elastic-plastic constitutive model.

## SAND LIQUEFACTION AND FLOW CONDITION

Seismic liquefaction refers to a sudden loss in stiffness and strength of soil due to cyclic loading effects of an earthquake. The loss arises from a tendency for soil to contract under cyclic loading, and if such contraction is prevented or curtailed by the presence of water in the pores that cannot escape, it leads to a rise in pore water pressure and a resulting drop in effective stress. If the effective stress drops to zero (100% pore water pressure rise), the strength and stiffness also drop to zero and the soil behaves as a heavy liquid. However, unless the soil is very loose (e.g. Dr $\leq$ 20 %) it will dilate and regain some stiffness and strength, as it strains. If this strength is sufficient, it will prevent a flow slide from occurring, but may still result in excessive displacements commonly referred to as lateral spread.

The excess pore water generated by seismic loading generally drains upwards, and if no barrier layers are present, dissipation results in a decrease in void ratio and an increase in strength and stability. The potential for lateral spreading and flow slides can greatly increase if low permeability layers e.g. silt layers within a soil deposit impede drainage, forming a barrier to flow that can result in an expansion of the sand skeleton (void redistribution) and accumulation of pore water at the base of the layers. If

the inflow to any element exceeds its ability to expand, the excess water will form a water film beneath the barrier layer resulting in a zone of zero shear strength.

Although a large number of laboratory investigations on liquefaction resistance of sands have been carried out, most of them dealt with undrained condition (constant volume) behavior. Recent laboratory studies, (e.g. Vaid & Eliadorani, 1998; Eliadorani, 2000) demonstrated that a small net flow of water into an element (injection) causing it to expand, resulted in additional pore pressure generation and further reduction in strength. Chu & Leong (2001) reported that the same phenomenon occurs in loose and dense sand, and called it pre-failure instability. Vaid & Eliadorani (1998) examined this phenomenon by injecting or removing small volumes of water from the sample using monotonic triaxial testing as it was being sheared and referred to this as a "partially drained condition" (this testing method is also called "strain path" e.g. Chu & Leong 2001). The results of inflow tests on Fraser River sand shown in figure 1 in terms of stress path, axial strain vs. time and strain path (with $Dr_c$= 29%) indicate a potential for triggering liquefaction at constant shear stress ($\sigma'_1 - \sigma'_3 =$ constant). Small imposed expansive volumetric strains resulted in effective stress reduction and flow failure of samples of sand consolidated to an initial state of stress corresponding to $R_c = \sigma'_{1c}/\sigma'_{3c} = 2$, as shown in Figure 1b, where $R_c$ is the consolidation effective stress ratio and $\sigma'_{1c}$ and $\sigma'_{3c}$ are the major and minor principle effective stresses respectively. They defined this condition as instability that occurs when a soil element subjected to small effective stress perturbation cannot sustain the current stress state and results in runaway deformation as seen in Figure 1c &1d, or liquefaction flow. As may be seen from Figure 1d the sample with $\sigma'_{3c}$ = 100 kPa failed once volumetric strain ($\varepsilon_v$) reached by 0.2%. In these tests, expansive $\varepsilon_v$ were imposed by injection of water into the samples (see Figure 1a) at a constant rate $d\varepsilon_v/d\varepsilon_1 = -0.4$, where $\varepsilon_1$ is the axial strain. The samples were stable under the initial stress state. The stress paths followed during injection indicate a reduction in effective stresses at a constant shear stress. At each initial confining stress, the stress changes leading to instability occurred with little change in shear stress and void ratio and at very small $\varepsilon_1$ of the order of 0.1%. Positive pore pressures continued to develop even beyond the phase transformation line. This occurs because the rate of imposed expansive volumetric strain is greater than the tendency for the skeleton to expand.

Yoshimine et al. (2006), Sento et al. (2004) and Bobei & Lo (2003) have reported similar response for Toyoura sand, and silty sand respectively. As a result, soil elements can liquefy due to expansive volumetric strains that cannot be predicted from analyses based on the results of undrained tests. To investigate the effects of low permeability layers on ground deformations due to earthquakes, it is necessary to predict the generation, redistribution, and dissipation of excess pore pressures during and after earthquake shaking. A fundamental approach requires a dynamic coupled stress-flow analysis. In such an analysis, the volumetric strains are controlled by the compressibility of the pore fluid and flow of water through the soil elements. To predict the instability and liquefaction flow, an effective stress approach based on an elastic–plastic constitutive model (*UBCSAND*) was used. The model is calibrated against laboratory element data as well as centrifuge data and is described below.

## CONSTITUTIVE MODEL FOR SANDS

The *UBCSAND* constitutive model is based on the elastic–plastic stress–strain model proposed by Byrne et al. (1995), and has been further developed by Beaty & Byrne (1998) and Puebla (1999). The model has been successfully used in analyzing the CANLEX liquefaction embankments (Puebla et al., 1997) and predicting the failure of Mochikoshi tailings dam (Seid-Karbasi & Byrne 2004b). It has also been used to examine partial saturation condition on liquefiable soil response (Seid-Karbasi & Byrne, 2006c) and dynamic centrifuge test data (e.g. Byrne et al., 2004 and Seid-Karbasi et al., 2005). It is an incremental elastic–plastic model in which the yield loci are lines of constant stress ratio ($\eta = \tau / \sigma'$). The flow rule relating the plastic strain increment directions is non-associated and leads to a plastic potential defined in terms of dilation angle as shown in Figure 2.

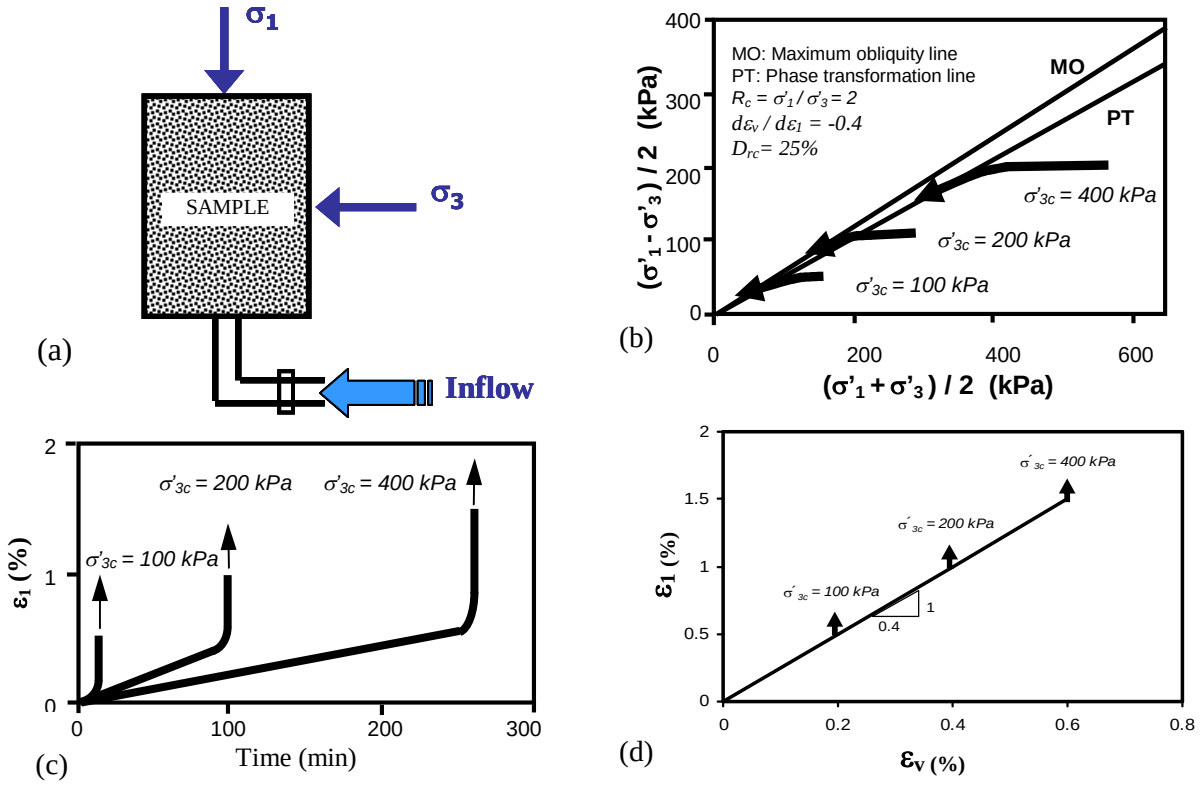


**Figure 1. Partially drained instability of loose Fraser River sand (data from Vaid & Eliadorani 1998): (a) inflow into traixial sample (b) stress paths; (c) strain paths and (d) axial strain vs. volumetric strain.**

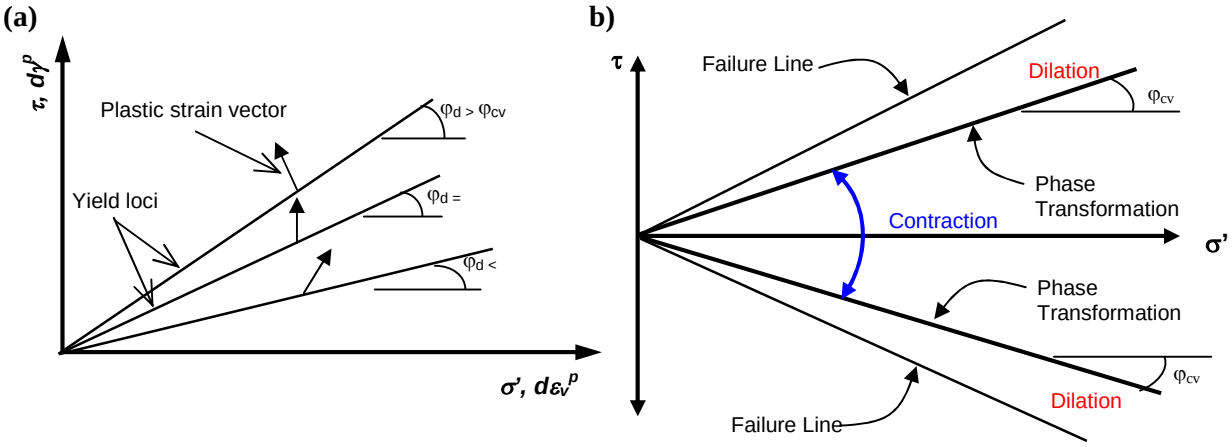


**Figure 2. (a) moving yield loci and plastic strain increment vectors, (b) dilation and contraction regions.**

The elastic component of response is assumed to be isotropic and specified by a shear modulus, $G^e$, and a bulk modulus, $B^e$, as Eq. 1 and Eq. 2, where $K^e_G$ is a shear modulus number, $P_a$ is atmospheric pressure, $\sigma' = (\sigma'_x + \sigma'_y) / 2$, $n_e$ is an elastic exponent approximately 0.5, $\alpha$ depends on elastic Poisson's ratio (varies from 0 to 0.2 as suggested by Hardin & Drnevich, 1972 and Tatsuoka & Shibuya 1992) and ranges from 2/3 to 4/3. The plastic shear strain increment $d\gamma^p$ and plastic shear modulus are related to stress ratio, $d\eta$ ($\eta = \tau / \sigma'$) as expressed by Eq. 3:

$$G^e = K_G^e . P_a \left( \frac{\sigma'}{P_a} \right)^{n_e} \quad (1) \qquad B^e = \alpha . G^e \quad (2)$$

$$d\gamma^p = \left( \frac{d\eta}{\left( \frac{G^p}{\sigma'} \right)} \right) \quad (3a) \qquad G^p = G_i^p \left( \left( 1 - \frac{\eta}{\eta_f} \right) R_f \right)^2 \quad (3b)$$

where $G^P$ is the plastic shear modulus and given by a hyperbolic function as Eq. 3b, $G^P_i$ is the plastic shear modulus at low stress ratio level ($\eta = 0$), $\eta_f$ is the stress ratio at failure and equals $sin\varphi_f$, where $\varphi_f$ is the peak friction angle, and $R_f$ is the failure ratio. The associated increment of plastic volumetric strain, $d\varepsilon_v^P$, is related to the increment of plastic shear strain, $d\gamma^P$, through the flow rule as follows:

$$d\varepsilon_v^P = d\gamma^P . (sin\varphi_{cv} - \eta) \quad (4)$$

where $\varphi_{cv}$ is the friction angle at constant volume (phase transformation). It may be seen that at low stress ratios ($\eta = \tau / \sigma' = sin\varphi_d$) significant shear induced plastic compaction is occurring, while no compaction is predicted at stress ratios corresponding to $\varphi_{cv}$. For stress ratios greater than $\varphi_{cv}$, shear induced plastic expansion or dilation is predicted.

This model was incorporated in the commercially available computer code FLAC (Fast Lagrangian Analysis of Continua) Version 5.0 (Itasca, 2005). This program models the soil mass as a collection of grid zones or elements and solves the coupled stress-flow problem using an explicit time stepping approach.

The key elastic and plastic parameters can be expressed in terms of relative density, *Dr*, or normalized Standard Penetration Test values, $(N1)_{60}$. Initial estimates of these parameters have been approximated from published data and model calibrations. The response of sand elements under monotonic and cyclic loading can then be predicted and the results compared with laboratory data. In this way, the model can be made to match the observed response over the range of relative density or N values. The model has also been calibrated to reproduce the NCEER 97 chart, which in turn is based on field data during past earthquakes and is expressed in terms of normalized Standard Penetration Test, $(N1)_{60}$ value. The model properties to obtain such agreement are therefore expressed in terms of $(N1)_{60}$ values.

**Model Simulation of Laboratory Element Tests**

The model was applied to simulate cyclic simple shear tests under undrained condition. Figure 3 shows model predictions along with test results on Fraser River sand. The test had an initial vertical consolidation stress $\sigma'_v$ = 100 kPa and *Dr* = 40%. The results in terms of stress-strain and excess pore pressure ratio, *Ru* and stress path compare reasonably well with the laboratory data. It should be noted that as unloading is considered elastic the excess pore pressure is constant while unloading takes place during cyclic shearing. A comparison of model prediction with tests results in terms of required number of cycles to trigger liquefaction for different cyclic stress ratios, *CSR* is shown in Figure 3c and shows reasonable agreement. The predicted stepped nature of the excess pore pressure rise with number of cycles occurs because the cycle count is updated at every half cycle. The pore pressure itself is computed at every step.

The model was also used to predict the effect of both undrained and partial drainage as observed in triaxial monotonic tests. The partial drainage involved injecting the sample with water to expand its volume as it was sheared. The injection causes a drastic reduction in strength. In the numerical model

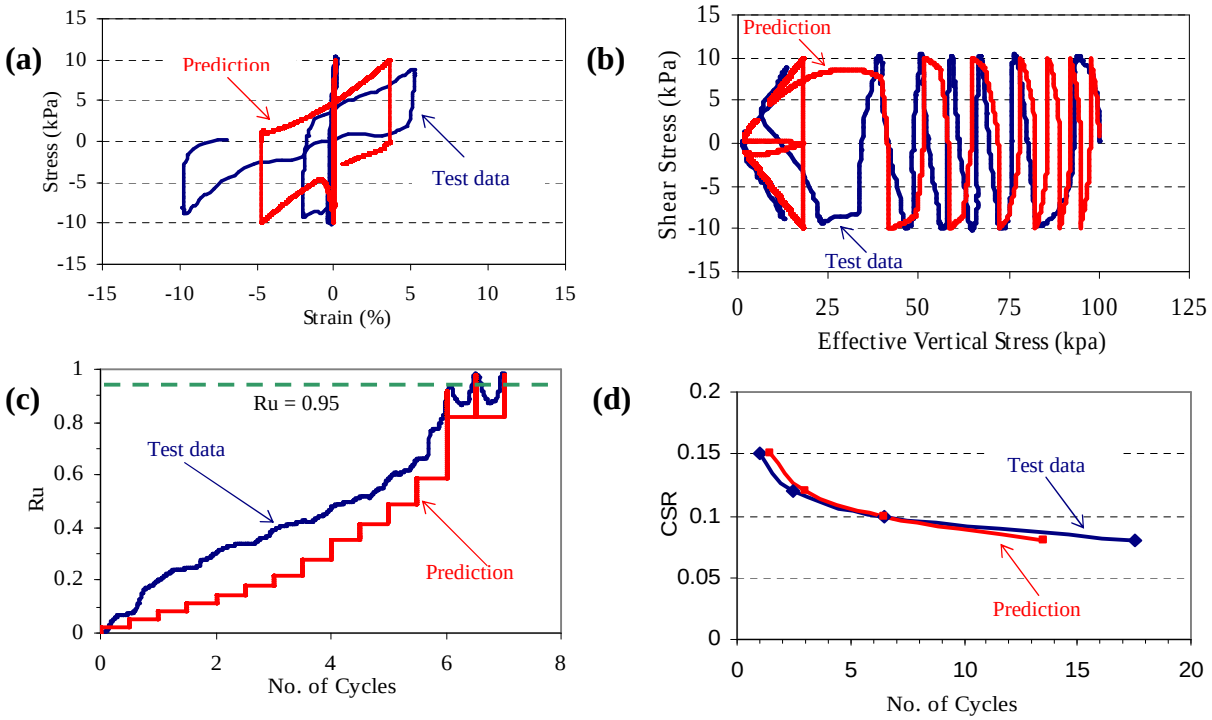


**Figure 3. Comparison of predicted and measured response for Fraser River Sand, $D_r$ = 40% & $\sigma'_v$ = 100 kPa (a) stress-strain, *CSR* = 0.1, (b) $R_u$ vs. No. of cycles (liquefaction: $R_u \geq 0.95$), (c) *CSR* vs. No. of cycles for liquefaction (tests data from Sriskandakumar, 2004).**

the same volumetric expansion was applied and the results shown in Figure 4 (model prediction with solid line) are in remarkably good agreement with the measured data. The above simulations illustrate that the model can generate the appropriate pore pressures and stress strain response to undrained loading as well as account for the effect of volumetric expansion caused by inflow of water into an element.

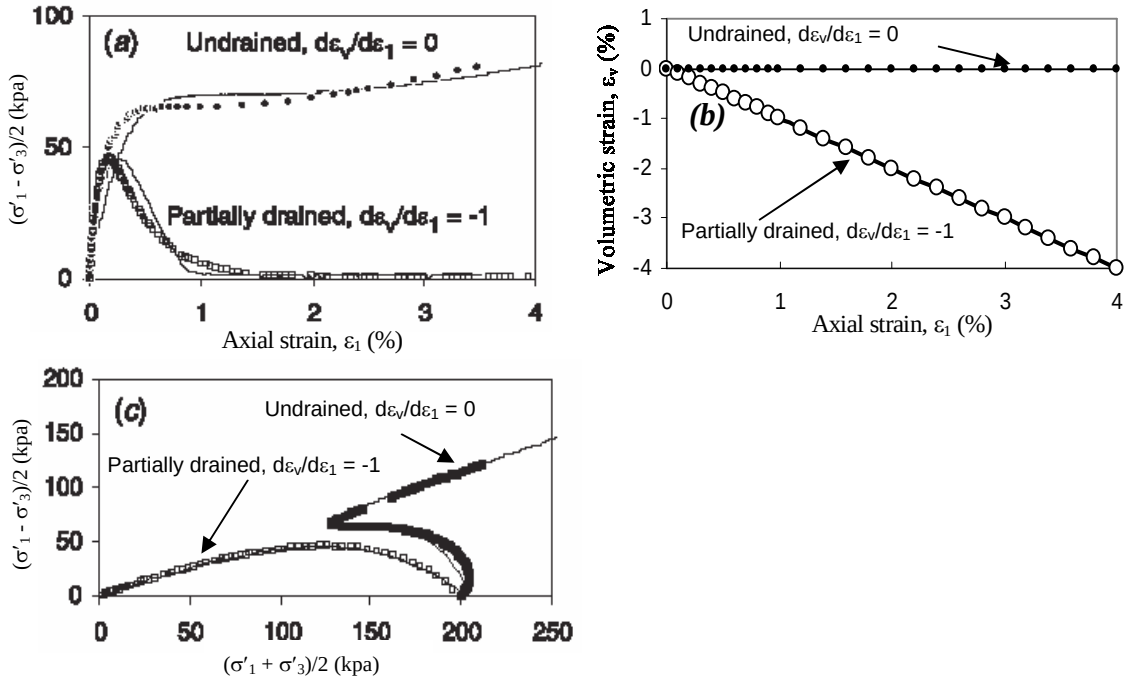


**Figure 4. Soil element response in undrained and partially drained (inflow) triaxial tests for FR River sand, (a) stress-strain, (b) volumetric strain, and (c) stress paths (modified from Atigh & Byrne 2004).**

## ANALYZED SOIL PROFILE

The soil profile used in this study is a 10 m thick deposit representing a sloping ground of 1° inclination with water table at surface as shown in Figure 5. It comprises of a loose sand deposit resting on an impermeable rigid foundation. The effect of a low permeability layer within the loose sand at a depth of 4 m is examined. Fraser River sand, with relative density *Dr* = 40 % is considered to represent the loose sand. Material properties are listed in Table 1, in which $\rho_d$, *n* and *k* are material dry density, porosity and permeability respectively. *UBCSAND* model was applied to the loose sand layer with corresponding equivalent *UBCSAND* $(N_1)_{60}$ value. The low permeability silt layer barrier is simulated with a Mohr-Coulomb model having friction angle, $\varphi$ = 30° and permeability, *k* one thousand times lower than that of the loose sand layer. Its stiffness in terms of bulk modulus and shear modulus was modeled as 1e4 kPa and 0.5e4 kPa respectively.

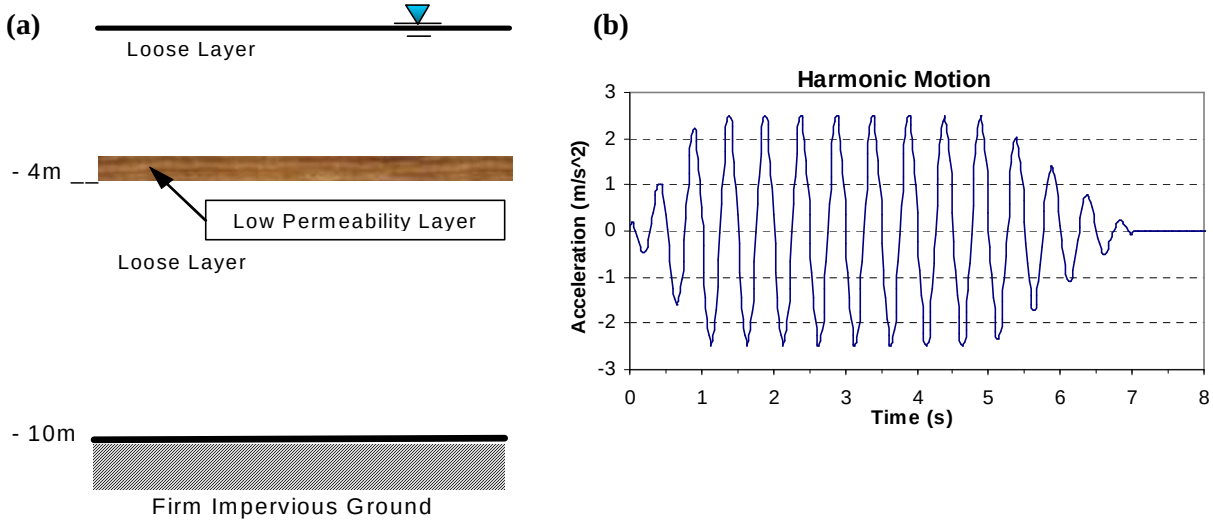


**Figure 5. (a) analyzed soil profile with barrier, (b) acceleration time history for input base motion.**

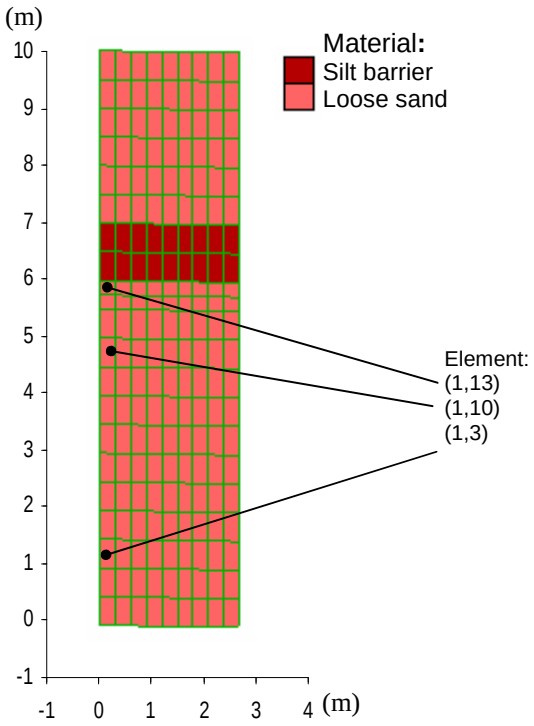


**Table 1**. Materials properties used in the analyses.

| Material | $\rho_d$ ($_{1000\ kg/m^3}$) | n | UBCSAND $N_{1(60)}$ | k (m/s) |
|---|---|---|---|---|
| Loose 40% | 1.50 | 0.448 | 6.2 | 8.81e-4 |
| Silt barrier | 1.50 | 0.448 | ---- | 8.81e-7 |

**Figure 6. Model of 10m-soil profile used in the analyses and selected points positions.**

It is not considered to generate excess pore pressure. Input base motion in terms of an acceleration time history is shown in Figure 5b. It is a harmonic (sinusoid) excitation applied at the base of the soil layer. It ramps up to 2.5 m/s$^2$ within 1s and dies out in 2s and lasts for 7s in total.

## ANALYSES RESULTS

To model the soil profile a mesh with 9 x 22 zones as illustrated in Figure 6 was used. Material types are recognized with different permeability values as shown in the figure. The nodes on the left and right boundaries were linked so as to force the soil column to deform as a shear beam. The earthquake motion was applied as a time history of acceleration at the base of the mesh. The time histories of excess pore pressure ratio, $R_u$ at different depths are shown in Figure 7. Pore pressures increase very rapidly, however beneath the barrier layer they remain high ($R_u \approx 100\%$) after the end of shaking, while dissipation occurs at greater depths. This indicates that water flows from the greater depths towards the layer beneath the barrier causing higher excess pore pressure to last for a significantly longer time compared to the case without a barrier. The injected flow causes an expansion of the layer beneath the barrier to occur at essentially zero effective stress and leads to large deformation during and after cease of shaking. Figure 8 shows the distorted mesh indicating localized deformation beneath the barrier layer. Such behavior has been reported from a number of centrifuge tests (e.g. Kulasingam et al., 2004 and Malvick et al., 2005) and examined in detail by Seid-Karbasi & Byrne (2007). Figure 9 shows the predicted isochrone of volumetric strain at 30 sec. within the soil deposit beneath the barrier layer. As may be seen the pore water redistribution results in contraction in the lower part of the soil profile while expansion is occurring in the upper (about 40%) of the profile. In the next section the effect of soil profile thickness in this characteristic behavior is discussed.

### Effect of Layer Thickness

*a) Total Soil Profile Thickness*

To investigate scale effects on predicted characteristic behavior of liquefiable grounds with sub-layer barrier, a separate series of analyses were conducted for the same soil profile shown on Figure 5. The problem was modeled in two different ways:

1. As a 10 m soil profile in 1 g-field (prototype scale) and
2. As a 0.1 m soil profile in 100 g-field (model scale) following appropriate conversion laws for modeling described by Schofield (1981) and Kutter (1995).

It is noted that the mesh size used in modeling (2) was one hundredth that used in modeling (1). The base input motion and mechanical properties of materials were the same as used before. The displacement patterns were identical for both models when examined in prototype scale and the same as shown in Figure 8. The profiles of volumetric strain beneath the barrier layer for both models were also identical and same as depicted on Figure 9. This suggests that for a soil profile comprising a barrier layer, contraction at the lower parts and expansion at the upper parts are characteristic behavior that occur due to pore water migration that result in void redistribution regardless of layer size. These findings indicate that the phenomenon of pore water redistribution can be captured in centrifuge tests and that the actual physical size of the layers is not important.

*b) Liquefiable Soil Layer Thickness*

Further studies were undertaken to analyze the problem under the same conditions (barrier layer at 4m depth) but using a 12m thickness for the liquefiable layer compared to a 6m thickness as used in the previous case. The pattern of deformation was the same as shown in Figure 8 with localization beneath the barrier layer. This can be better seen when the depth is normalized with respect to liquefiable layer thickness as shown in Figure 10. As may be seen the volume change isochrones are practically identical indicating that compression occurs in the lower part (about 60%) of the liquefiable layer while it expands in the upper part (about 40%). This indicates that the pattern of volumetric strain (void redistribution) is essentially the same for similar drainage conditions

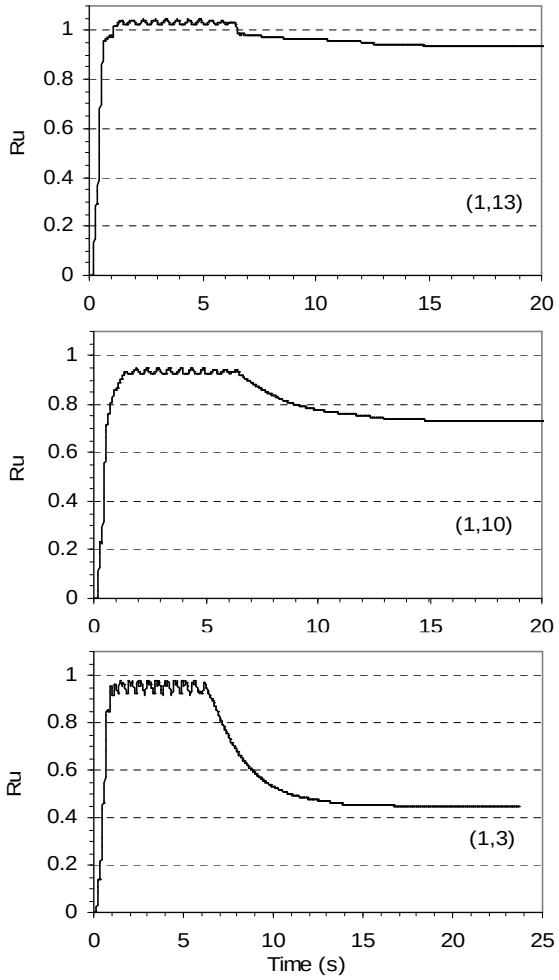


**Figure 7. Time histories of excess pore pressure ratio, *Ru* for selected points below the barrier (Seid-Karbasi & Byrne, 2006b).**

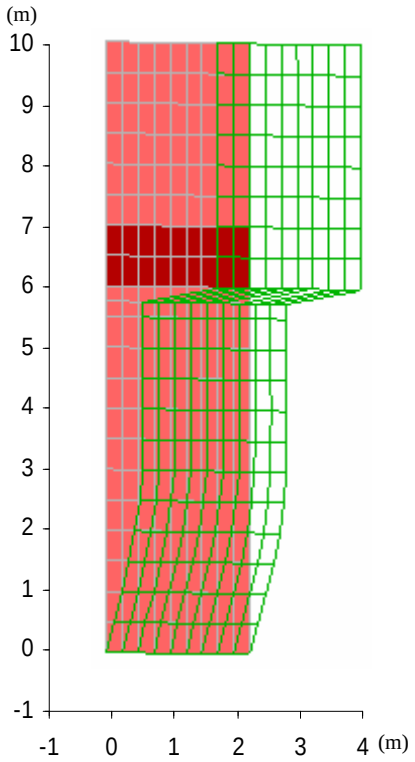


**Figrue 8. Deformation pattern of soil profile with barrier (Seid-Karbasi & Byrne, 2006b).**

regardless of layer thickness. This finding was counter intuitive as our expectation was that a thicker liquefiable layer would lead to greater expansion.

## DISCUSSION

The concept of reduced strength resulting from void expansion is consistent with critical state concepts. Consider an element of sand beneath a slope of liquefiable soil with a barrier sub-layer. The effective stress versus void ratio path followed by such an element is examined in Fig 11. The initial in situ state is defined as $A_0$ with void ratio $e_0$. If shaking takes place in an undrained or constant volume state the point will move to location $A_1$ with essentially zero effective stress but the same void ratio, $e_0$, when liquefaction is triggered. At this in situ void ratio the element would have an undrained strength corresponding to point $A_2$ on the critical state line in Fig11. This strength would be greater than the drained strength. Thus there is no danger of flow failure during or following seismic loading if the element remained at the in situ void ratio, $e_0$. If void redistribution occurs largely after liquefaction is triggered then expansion takes place at approximately zero effective stress. If expansion is sufficient, the element may reach the critical state at essentially zero effective stress and zero strength, corresponding to point $A_3$. At this point the skeleton has no further ability to expand, and further inflow to the element will result in the formation of a water film or bubble as observed in 1D Colume tests by Kokusho (2003) representing a level ground condition.. Thus for stratigraphic

conditions corresponding to layered sands and silts, sand elements beneath the silt could have a strength ranging from the undrained strength to zero depending on their density and the severity of earthquake shaking. This explains why strengths obtained from back analysis of case histories can be so much lower than the undrained strength.

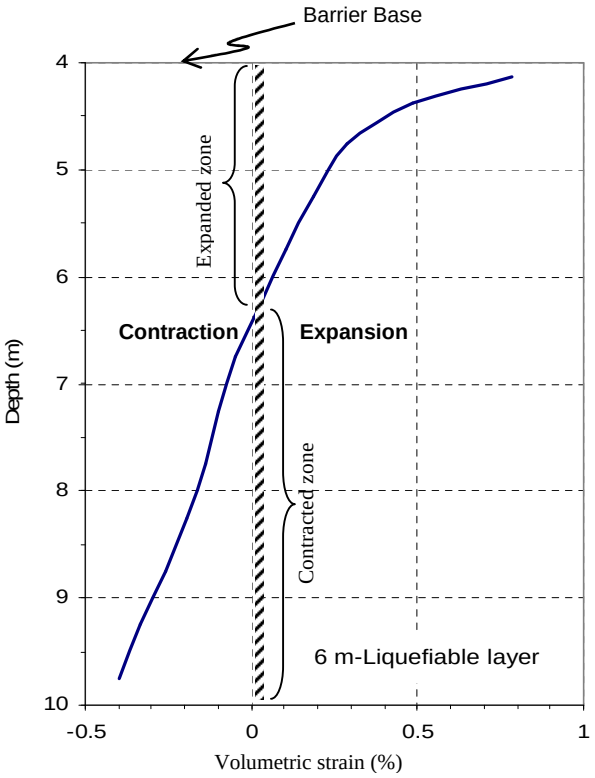


**Figure 9. Volumetric strain isochrone beneath the barrier layer, after 30s (6m liquefiable layer) (Seid-Karbasi & Byrne, 2007).**

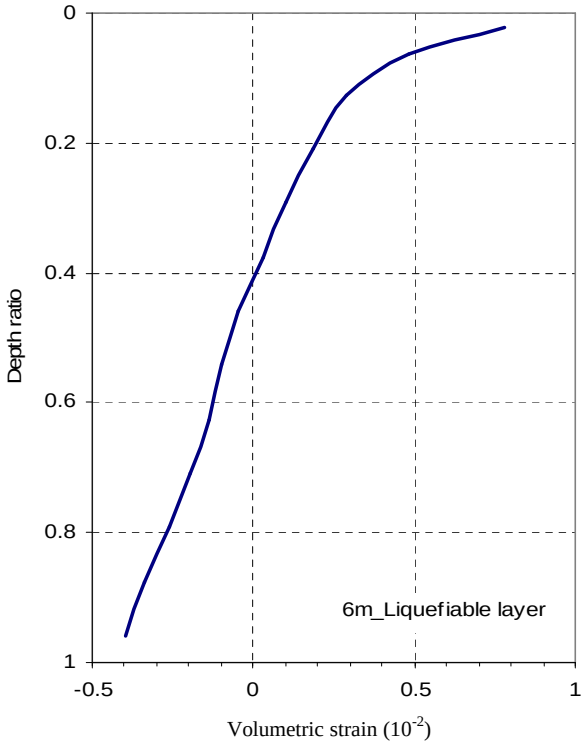


**Figure 10. Volumetric strain isochrone for the profile of 12m liquefiable layer.**

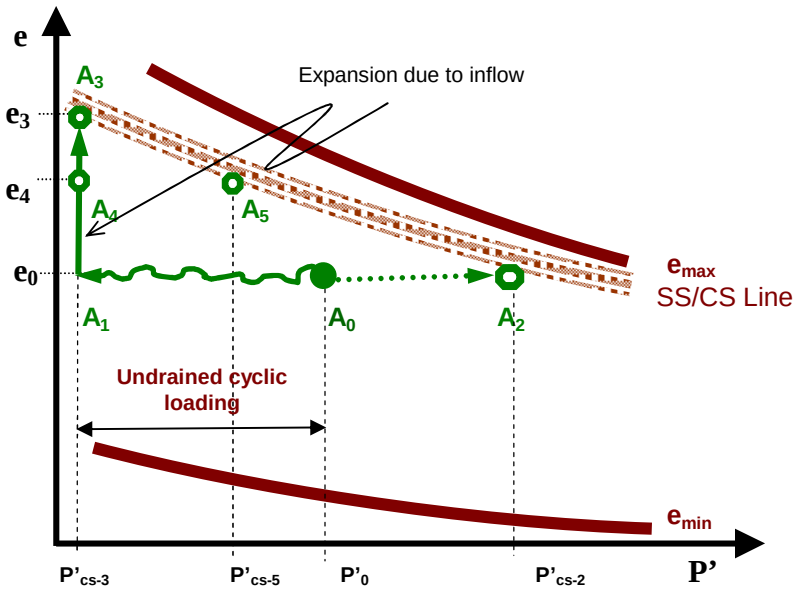


**Figure 11. Void ratio and effective stress change at the barrier base due to undrained shaking and pore pressure redistribution.**

## CONCLUSIONS

The seismic response of earth structures is controlled by two key factors i.e. mechanical conditions and flow conditions. The presence of a low permeability sub-layer can have a significant impact on liquefiable ground response resulting in large displacements with localization beneath the barrier layer due to impedance of flow path during and after shaking. A dynamic stress-flow coupled analysis procedure was employed to investigate the characteristic behavior of an infinite slope with barrier layer. It was shown that in a liquefiable soil layer with a barrier layer, pore water redistribution results in the formation of an expansion zone beneath the barrier, while contraction occurs in the lower parts. The numerical modeling procedure predicts that the barrier layer effect is a characteristic feature of liquefiable slopes and is independent of liquefied soil layer thickness.

It has been common to assume that the residual strength available to prevent a flow slide from occurring is an undrained strength. Back analyses of field case histories indicate that the residual strength can be much lower than the undrained strength from testing undisturbed laboratory samples. Both dynamic centrifuge and shaking table tests as well as coupled stress-flow analyses demonstrate that the lower than expected residual strength is due to void expansion associated with barrier layers.

## REFERENCES


Atigh, E. and Byrne, P. M. "Liquefaction flow of submarine slopes under partially undrained conditions: an effective stress approach," *Can. Geotechnical J*., V. 41, pp. 154-165, 2004.

Beaty, M. H. and Byrne, P. M. "An effective stress model for predicting liquefaction behavior of sand," *Proc., Conf., Geotech.Eq.Engg. & Soil Dyn.III*, ASCE GSP No. 75, V1, pp. 766-777, 1998.

Bobei, D.C., and Lo, S-C. "Strain path influence on the behavior of sand with fines," *Proc.,12th Pan.Conf.,Soil Mechanics and Geotech.Engg.*, MIT, Massachusetts, pp. 583-588, 2003.

Chu, J. and Leong, W. K. "Pre-failure strain softening and pre-failure instability of sand: a comparative study," *J. Geotechnique*, V. 51, No. 4, pp. 311-321, 2001.

Byrne, P.M., Roy, D., Campanella, R.G., and Hughes, J. "Predicting liquefaction response of granular soils from pressuremeter tests," *ASCE National Convention, ASCE, GSP 56*, pp. 122-135, 1995.

Byrne, P.M., Park, S., Beaty, M., Sharp, M., Gonzalez, L. and Abdoun, T. "Numerical modeling of liquefaction and comparison with centrifuge tests," *Can. Geotech. J.*, V. 41, pp. 193-211, 2004.

Eliadorani, A. "The response of sands under partially drained states with emphasis on liquefaction," *PhD.Thesis, Civil Engg.* Dept., the University of British Columbia, Vancouver, B.C., 2000.

Elgamal, A. W., Dobry, R., and Adalier, K. "Small scale shaking table tests of saturated layered sand-silt deposits", *Proc., 2nd U.S.-Japan Workshop on Soil Liquefaction*, Buffalo, N.Y., NCEER Rep. No. 89-0032, pp. 233–245, 1989.

Hamada, M. "Large ground deformations and their effects on lifelines: 1964 Niigata Earthquake," *Proc.,Lifeline Performance During Past Earthquakes*, V. 1: Japanese Case Studies Tech. Rep. NCEER-92-0001, NCEER, Buffalo, N.Y., 3/1–3/123, 1992.

Hardin, B. and Drnevich, V. "Shear modulus and damping in soils: Deign equations and curves", *J., Soil Mech., & Found. Engg., ASCE*, V. 98, pp. 667-692, 1972.

ITASCA, Fast lagrangian analysis of continua (FLAC), Version 5, *User's Guide.* Itasca Consulting Group, Inc, 2005.

Kokusho, T. "Water film in liquefied sand and its effect on lateral spread," *Journal of. Geotechnical and Geo-Environmental Engineering, ASCE,* V. 125, pp. 817–826, 1999.

Kokusho, T. and Kojima, T. "Mechanism for post-liquefaction water film generation in layered sand," *J., Geotechnical and Geo-Environmental Engineering, ASCE,* V. 128, pp. 129–37, 2002.

Kokusho, T. Current state of research on flow failure considering void redistribution in liquefied deposits. *J., Soil Dynamics and Earthquake Engineering,* V. 23, pp. 585–603, 2003.

Kulasingam, R., Malvick E. J., Boulanger, R. W. and Kutter, B. L. "Strength loss and localization at silt interlayers in slopes of liquefied sand," *J.,Geotech., & Geoenviron.Engg., ASCE,* V. 130, pp. 1192-1202, 2004.

Kutter, B. L. "Recent advances in centrifuge modeling of seismic shaking," *In Proc., 3rd Int. Conf., Recent Advances in Geotechnical Earthquake Engineering and Soil Dynamics*, University of Missouri–Rolla, Mo., V. 2, pp. 927–942, 1995.

Malvick, E. J., Kutter, B. L., Boulanger, R. W., Kabasawa, K. and Kokusho, T. "Void redistribution research with 1-g and centrifuge modeling," *In Proceedings of Int. Con. Soil Mech. Geotehnical Engg.*, ISSMGE. Osaka, V. 4, pp. 2543-2546, 2005.

Puebla, H."A constitutive model for sand analysis of the CANLEX embankment," *PhD. Thesis, Civil Engg. Dept.*, Un., British Columbia, Vancouver, B.C. 1999.

Puebla, H., Byrne, P. M., and Phillips, R. "Analysis of CANLEX liquefaction embankment: prototype and centrifuge models," *Canadian Geotechnical J*., 34, pp. 641-654, 1997.

Schofield, A. N. "Dynamics and earthquake geotechnical centrifuge modeling," *In Proc., Int. Conf., Recent Advances in Geotechnical Earthquake Engineering and Soil Dynamics*, University of Missouri–Rolla, Mo., V. 3, pp 1081–1100, 1981.

Scott, R. F., and Zuckerman, K. A. "Sand blows and liquefaction in the Great Alaskan Earthquake of 1964," *Engineering Publication 1606*; National Academy of Sciences, Washington, D.C., pp 170-189, 1972.

Seid-Karbasi, M., Byrne, P. M. "Liquefaction, lateral spreading and flow slides," *In Proc. 57th Canadian Geotechnical. Conf.*, p. G13.529, 2004a.

Seid-Karbasi, M. and Byrne, P. M. "Embankment dams and earthquakes," *Hydropower and Dams J*., V.11(2), pp. 96-102, 2004b.

Seid-Karbasi, M., Byrne, P. M., Naesgaard, E., Park, S., Wijewickreme, D., and Phillips, R. "Response of sloping ground with liquefiable materials during earthquake: a class A prediction," *In Proc., 11th Int. Conf., Int. Ass., Computer Methods & Advances in Geomechanics, IACMAG*, Turin, Italy, V. 3, pp. 313-320, 2005.

Seid-Karbasi, M., and Byrne, P. M. "Significance of permeability in liquefiable ground response," *In Proc. 59th Canadian Geotechnical. Conf.*, pp. 580-587, 2006a.

Seid-Karbasi, M., and Byrne, P. M. "Seismic liquefaction, lateral spreading and flow slides: A numerical investigation into void redistribution," Accepted by *Canadian Geotechnical J, 2007.*

Seid-Karbasi, M., and Byrne, P. M. "Effects of partial saturation on liquefiable ground response", *In Proc., ASCE 2006 Geo-Congress, Geotechnical Engineering in Information Tech. Age*, Atlanta, Ga., Paper # 11803, 2006c.

Sento, N., Kazama, M., Uzuoka, R., Hirofumi Ohmur H., and Makoto Ishimaru, M. "Possibility of post liquefaction flow failure due to seepage," *J., Geotechnical and Geoenvironmental Engineering, ASCE*, V. 130, pp. 707-716, 2004.

Sharp, M., Dobry, R. Abdoun, T. "Liquefaction centrifuge modeling of sands of different permeability," *J., Geotechnical and Geoenviron. Engg., ASCE*, V. 129, pp. 1083-1091, 2003.

Sriskandakumar, S. "Cyclic loading response of Fraser River Sand for numerical models simulating centrifuge tests", *M.A.Sc. Thesis*, the University of British Columbia, Vancouver, B.C., 2004.

Tatsuoka, F. and Shibuya, S. "Deformation characteristics of soils & rocks from field and lab tests," *Report of the Institute of Industrial Science 37* (1), Setial No. 235, Uninvesity of Tokyo, 136p.

Vaid, Y. P., and Eliadorani, A. "Instability and liquefaction of granular soils under undrained and partially drained states," *Canadian Geotechnical J.*, V. 35, pp. 1053–1062, 1998.

Yang, Z., and Elgamal, A. "Influence of permeability on liquefaction-induced shear deformation", J., Engineering Mechanics, ASCE, V. 128, pp. 720-729, 2002.

Yoshimine, M., Nishizaki, H., Amano, K. and Hosono, Y. "Flow deformation of liquefied sand under constant shear load and its application to analysis of flow slide of infinite slope," *J., Soil Dynamics and Earthquake Engineering*, V. 26, pp. 253-264, 2006.

Youd, T. L., Idriss, I. M., Andrus, R., Arango, I., Castro, G., Christian, J., Dobry, J., Finn, L., Harder Jr., L., Hynes, H. M., Ishihara, K., Koester, J., Liao, S. S., Marcuson III, W. F., Martin, G., Mitchell, J. K., Moriwaki, Y., Power, M. S., Robertson, P. K., Seed, R. B., and Stokoe II, K. H. "Liquefaction Resistance of Soils: Summary Report from the 1996 NCEER and 1998 NCEER/NSF Workshops on Evaluation of Liquefaction Resistance of Soils", *J., Geotech. and Geoenviron. Engg., ASCE*, V. 127, pp. 817-833, 2001.